JOURNAL OF MATERIALS SCIENCE 33 (1998) 147–153

Determination of the true stress–strain behaviour of polypropylene

E. KONTOU, P. FARASOGLOU
Department of Engineering Science, Section of Mechanics, National Technical University of Athens, 5 Heroes of Polytechnion, GR-15773, Athens, Greece

The true tensile and compressive stress–strain curves for a typical semicrystalline polymer (polypropylene) were constructed with a new experimental technique. This is based on a non-contact method of strain measurement along the specimen gauge length. The viscoplastic behaviour obtained in this manner was then described with a nonlinear viscoelastic constitutive model mentioned analytically elsewhere. This consideration leads to a satisfactory description of yield and post yield behaviour, including strain softening, and strain hardening. The rate effect was also predicted with a high accuracy.

1. Introduction

Conventional tensile testing has been widely used to study the mechanical properties of solid polymers. However, only a small minority of plastic materials exhibit uniform extension at a constant rate tensile experiment. Very often, the initial Hookean elastic behaviour is followed by a non-uniform plastic deformation, which may have the form of a shear band, crazing or necking [1]. The early occurrence of necking in these tests leads to an inadequate physical interpretation of the quantities derived from the experimental data. As a consequence of this effect, the results provided by the experiment do not represent the true response of the material.

In order to provide the correct description of the mechanical behaviour of the material, the measurement of true stress and true strain in local terms is required.

On the other hand, the yield and post-yield behaviour of glassy polymers is widely known to exhibit several distinct characteristics. The initial yielding of the material depends on pressure, strain rate and temperature. After yielding the material appears to have the response of true strain softening, which is followed by a subsequent strain hardening.

The mechanism of yielding can be mainly defined by two different approaches. The first one is based on a possible analogy with the plasticity of metals. In this case, yielding is due to the initiation and propagation of defects of the type of dislocation [2]. According to the second approach, yielding in polymers is related to molecular relaxation processes, and it occurs when the plastic flow rate is equal to the applied strain rate.

The yield point of glassy polymers has been considered as a state where plastic flow begins. To study the molecular mechanism of this plastic flow, the application of the Eyring [3] equation has been tested. The yielding of polymethyl methacrylate (PMMA) [4] and polypropylene [5] has been analysed as a two stage process by Roetling using the Ree–Eyring equation [6].

Ngai *et al.* [7] have applied the coupling model of relaxation to non-linear viscoelasticity and have successfully described the stress response at a constant strain rate, step strain rate and stress relaxation of polycarbonate. Concerning the question of whether a structural change occurs at yielding, Shay and Caruthers [8] considered that the polymeric structure changes continuously during the yield process rather than making an abrupt transition from a solid to a liquid like structure at the yield point. Lefebvre and Escaig [9] proposed a contribution from the nucleation of molecular defects to the plastic strain and suggested an inhomogeneous structural change during yielding. The different mechanisms related to the yielding process (strongly affected by the physical ageing of polymer) are also discussed by Rudner *et al.* [10].

In the particular case of semicrystalline polymers, yielding and cold-drawing contain two types of non-uniform deformation processes: the first one is the initiation of local necking and the other is the propagation of neck shoulders along the specimen. Both types result from the local instability of deformation but they are different in behaviour [1]. The solid state rheology of polypropylene as a function of temperature was also studied by Duffo *et al.* [11]. Experimental stress–strain curves recorded in uniaxial tension at different strain rates by means of a video-controlled testing system were presented and modelled through a simple constitutive equation.

In this work, the yield and post yield behaviour of polypropylene, which is a typical semicrystalline polymer, will be tested in terms of tensile and compressive tests. Instead of the engineering stress–strain data, the true stress–strain curve will be obtained in terms of a new experimental technique.

This system permits a non-contact measurement of longitudinal deformation distribution on the sample,

0022–2461

while the load is recorded simultaneously. For a constant crosshead speed experiment, it has been found that the local strain rate appears to vary by one or two orders of magnitude. Therefore, the tensile stress had to be corrected for this strain rate variation, with the further assumption that the deformation procedure has an isovolume characteristic (the latter fact has been verified in the case of the same polymer type elsewhere [11]). In this way, the true stress–strain curves have been constructed for tensile and compression experiments at the three different crosshead speeds tested.

The theoretical description of the experimental results has been made successfully with a constitutive equation presented in detail in a previous publication [12]. According to this analysis, which is based on the work of Chow [13, 14], the prediction of yield behaviour is based on the concept of local configurational rearrangements of the molecular segments, which lead to different domain sizes due to the application of an external stress field. Following Chow's assumptions [14], the concept of an activation volume tensor has been related with the relaxation time, which has an important effect on the nonlinear viscoelasticity. The post yield behaviour has been predicted [12] by introducing a stress back tensor, while the parameter values are connected with the molecular structure of the material tested.

2. Experimental procedures

The polypropylene used in the present work is produced under the commercial name APPRYL 3020 BN1 (Elf Atochem), with a melt index equal to 1.9 g min^{-1}. It was processed into the shape of cylindrical extruded rods, 3.5 mm in diameter and free of bubbles. Dogbone shaped tensile specimens were then constructed with an average thickness of 3 mm and a gauge length of 30 mm. In order to erase any prehistory effects the samples were annealed in a vacuum oven (< 10 m Torr) at 15 °C above the glass transition temperature for 1 h. The samples then were allowed to cool at room temperature over a period of 8 h.

The tensile experiments were performed using an Instron 1121 tester at room temperature. Three different crosshead speeds were used, namely 0.1, 1 and 10 mm min^{-1}. The longitudinal strain could be measured very accurately, with the laser-extensometer which permits a non-contact measurement of the longitudinal deformation distribution of the samples.

The system is constructed according to the principles shown in Fig. 1a. A beam is cast by a laser onto a rotating mirror. By rotation of the seal the laser scans a tape pattern code which is applied on to the specimen. A special painting technique has been followed for the application of a deformable coating on the sample. The reflections of the tape patterns are registered by a photocell. The part of the sample to be measured is determined and limited by the opening in the case, as is shown in Fig. 1b. Due to the geometric arrangements the aperture θ is approximately 23°. During the rotation of the mirror and before leaving the case, the laser beam slips over the first photodiode

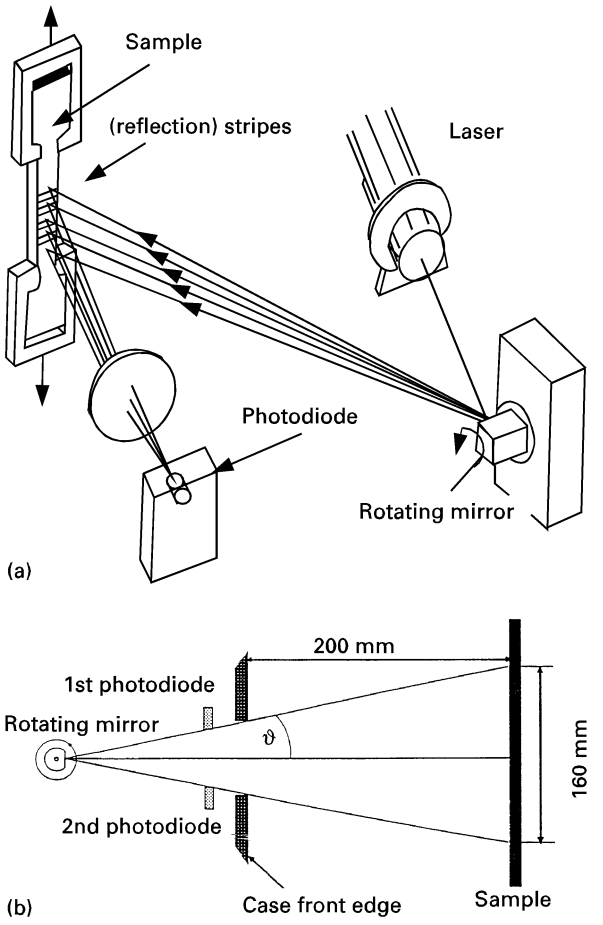

Figure 1 (a) Schematic presentation of the principle of the laser extensometer, and (b) measuring geometry of the test system.

which gives a start signal. After the scan a stop signal is given by the 2nd photodiode.

For the elongation measurements a contrasting tape pattern code was applied to the gauge length of the sample, namely fifteen white stripes on a dark background. The spacings between the stripes were 1 mm. From the gap between the first and last markings and the mirror speed, the calibration of the path length is taken as the middle value of the first scans. At the beginning (and end) of the scan a start (stop) signal is given. The actual elongation measurement is done via counting units.

The compression experiments were performed with the same Instron tester, at three different crosshead speeds of 0.1, 1 and 10 mm min^{-1}. Cylindrical specimens with a mean diameter of 9 mm and an average length of 18 mm were used. Care has been taken to ensure that the cylinder ends are smooth and parallel, while the problem of barrelling has been eliminated by using a thin sheet of Teflon between the specimen and the compression grip. An analogous pattern code to that used in the tensile samples was applied to the gauge length, in this case four stripes on dark background. The space between the individual stripes was 3 mm in order to permit the reflection of the laser beam during compression, during which a decrease in the space between the stripes occurs. A minimum of three tests were run at each strain rate.

During both the tensile and compression tests the load and strain were recorded simultaneously, with

the data acquisition being performed with a computerized system. The construction of engineering and true stress–strain curves was then made, as will be discussed below.

The experimental technique, used in the present work, has the advantage of giving a detailed description of the deformation distribution, as well as the corresponding strain rates along the gauge length of the material tested.

3. Results and discussion

In a series of recent papers by Chow [13, 14], it was shown that under an externally imposed stress field σ_{ij} in a polymeric system, the relaxation time τ has the form:

$$\tau = \tau_0 \exp\left[-\frac{\sigma_{ij}\omega_{ij}}{2\, fbRT} \right] \tag{1}$$

where τ_0 is the pre-exponential factor which depends on a reference relaxation time [12]. ω_{ij} is the activation volume component, while the ratio ω_{ij}/f expresses the volume of the polymer segment needed to move as a whole for plastic yield to occur, b denotes the shape of the relaxation spectrum, R is the gas constant and T is the temperature.

Yielding occurs when the product of the relaxation time and the applied strain rate reaches a constant value close to unity [3]:

$$\dot{e}\tau = \text{constant} \tag{2}$$

On the other hand, the relaxation modulus of glassy polymers may be given by the Kohlrausch, Williams, Watts (KWW) equation [15]:

$$E_{ijkl} = E^0_{ijkl} \exp\left[-\left(\frac{t}{\tau}\right)^b \right] \tag{3}$$

with b varying between 0 and 1, and E^0_{ijkl} being unrelaxed modulus.

The constitutive equation of non-linear viscoelasticity is given by:

$$\sigma_{ij}(t) = \int_0^t E_{ijkl}(t-s)\dot{e}_{kl}\, \mathrm{d}s \tag{4}$$

and following the analysis of our previous work we obtain:

$$\sigma_{ij}(e_{kl}) = E^0_{ijkl} \times \int_0^{e_{kl}} \exp\left[-\frac{e'_{kl} \exp\left(\dfrac{\sigma_{kl}(e_{kl} - B_{kl}(e_{kl})}{K_{kl}/2.303} \right)}{\dot{e}_{kl}\tau_0} \right] \mathrm{d}e_{kl} \tag{5}$$

where $\dot{e}_{kl}$ is the rate of deformation, e_{kl} is the deformation and K_{kl} the slope of the plot of the yield stress as a function of logarithmic strain rate. By taking into account Equations 1 and 2 this plot is a straight line over a wide range of strain rates. The term B_{kl} has been introduced as an internal variable, and defines the deformation resistance the material has to overcome, due to the molecular alignment occurring after yielding and stress overshooting. This molecular alignment results in a change in the configurational entropy of the system. The tensor B_{ij} is similar to that initially proposed by Haward and Thackray [16] that was extended to 3-D problems by Parks *et al.* [17].

Furthermore, it is assumed that the free energy change due to intra- and inter-molecular changes is negligible compared to the change of the configurational entropy, which is largely due to the orientation of the chains. Due to the rubbery network-like response of glassy polymers to plastic deformation [18, 19], back stress has been modelled using a statistical mechanics approach to the rubber elasticity, namely the Wang and Guth [20] model of rubber elasticity. Therefore, the stress can be expressed as:

$$\sigma_{ij} = Y + C_{\mathrm{R}} \frac{N^{1/2}}{3} \left[\lambda_i L^{-1} \frac{\lambda_i}{N^{1/2}} - \left(\frac{1}{3}\right) \sum_{j=1}^{3} \lambda_j L^{-1} \frac{\lambda_j}{N^{1/2}} \right] \tag{6}$$

where Y is the extrapolated yield stress, λ_i is the stretch ratio, λ_j the stretch ratio in the other principal direction, defined with the assumption of the isovolume deformation during yielding. C_{R} is the rubbery modulus and L^{-1} is the inverse Langevin approximation. N is the number of rigid chain links between physical molecular chain entanglements. The numerical evaluation of Equation 5 was made using the method previously described by Kontou [12].

To test the validity of Equation 5 tensile and compressive experimental data obtained on polypropylene were examined. The engineering tensile stress–strain curves are shown in Fig. 2, in which we have assumed that the stress σ_{a} can be obtained by dividing the load P by the original cross-sectional area A_0

$$\sigma_{\mathrm{a}} = \frac{P}{A_0} \tag{7}$$

at the three different crosshead speeds. These curves are typical of a cold draw material and are plotted in respect to that zone of the gauge length where plastic deformation and neck initiation occurs. As is shown in Fig. 2 the load reaches its maximum value after the initial elastic behaviour and then it falls to a lower value which remains almost constant until fracture occurs. The yielding and cold drawing of semicrystalline polymers contains two types of nonuniform deformation processes: one is the initiation of local necking and the other is the propagation of necking shoulders along the specimen. Therefore, the objective response of the material can be given only in terms of a true stress–strain curve. As has already been mentioned, the available experimental technique permits the detailed description of the deformation distribution for each of the fifteen successive zones. Therefore, it is possible to localize a specific zone, where the magnitude of the strain is much higher with respect to the other zones. The strain versus time behaviour in that specific zone, (labelled as the reference zone), for a tensile test with a crosshead speed of 0.1 mm min^{-1} is shown in Fig. 3, in terms of true strain following the relation $\varepsilon = \ln(1 + e)$, where e is the engineering strain. Also in Fig. 3 we show the time evolution of the

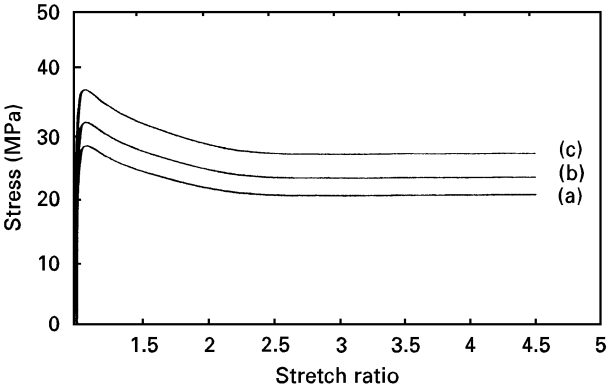

Figure 2 Engineering tensile stress–strain curves of polypropylene at crosshead speeds of (a) 0.1 mm min^{-1} (b) 1 mm min^{-1} and (c) 10 mm min^{-1}.

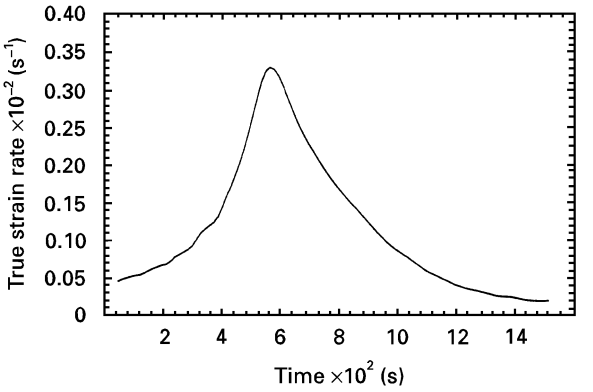

Figure 4 True strain rate versus time, for the reference zone with maximum deformation obtained from data of Fig. 3.

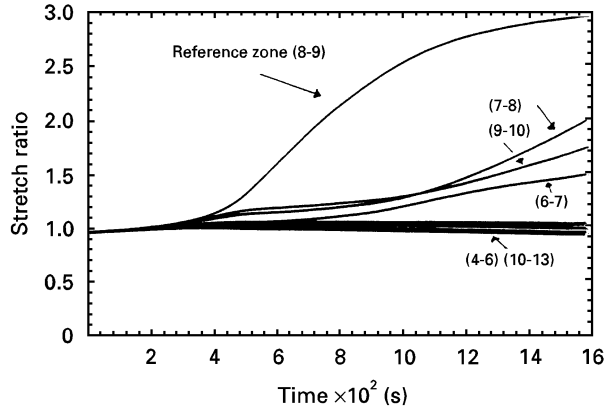

Figure 3 Strain variation versus time between ten successive zones, for a tensile test with a crosshead speed of 0.1 mm min^{-1}.

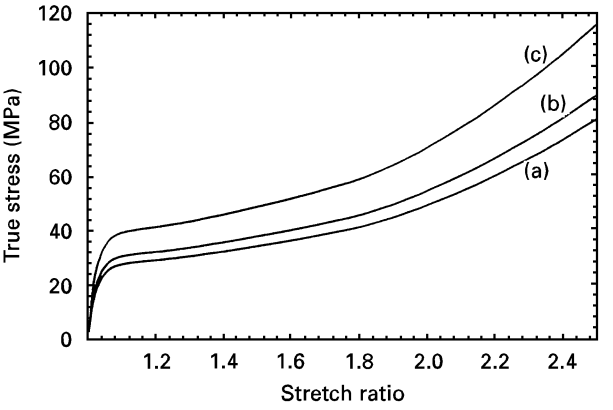

Figure 5 Tensile true stress–strain curves of polypropylene at crosshead speeds of (a) 0.1 mm min^{-1}, (b) 1.0 mm min^{-1} and (c) 10 mm min^{-1}.

strain distributed along ten successive zones, numbered from zone 4 to zone 13 of the specimen gauge length. These ten zones were selected so as to be equally spaced around the region where yield initiation takes place.

It can be observed that during the initial elastic response, all the zones have almost the same strain. Later, when yielding occurs followed by necking initiation at a specific zone (numbers 8 and 9), a large deviation of strain appears with respect to the rest of the regions, where a small decrease of strain takes place. This deviation appears to have a decreasing trend, when the neck propagation has completely passed through this specific zone, which extends into neighbouring regions. From the data of Fig. 3, the localized strain rate as a function of time for the zone of maximum strain can also be evaluated via:

$$\dot{\varepsilon} = \frac{1}{1+e}\frac{\mathrm{d}e}{\mathrm{d}t} \tag{8}$$

and the calculated data are presented in Fig. 4. From this figure it is observed that the strain rate is initially very slow and is almost equal to the imposed strain rate. Then in this specific zone it speeds up, reaching a peak and then decreases. This decrease is strong evidence for the development of strain hardening.

Assuming that the nonuniform deformation takes place under isovolume conditions, the true effective stress can be given by:

$$\sigma = \frac{P}{A} = \frac{(1+e)P}{A_0} = \sigma_a(1+e) \tag{9}$$

where A is the actual cross-section at any time. The true tensile stress–strain curves are shown in Fig. 5, and they exhibit a yield stress at a strain that is almost equal to 10%, while the effect of the strain rate on yield stress is obvious. No stress drop is observed after yielding, and at higher strains a subsequent strain hardening takes place.

From these results the yield stress as a function of the logarithmic rate of deformation plot can be obtained and it is shown as Fig. 6. The slope of this straight line corresponds to the magnitude of K_{kl} of Equation 5 and for the tensile tests it was found to have a value of 2.6 MPa. The intersect of this line gives an estimation of the pre-exponential factor τ_0 which was found to be equal to 6×10^8 s. The parameter N is equal to the terminal or locking strain as has been discussed by Boyce *et al.* [21]. The phenomenon of locking, recorded as a sharp upturn in the stress–strain curve reflects the increased difficulty in further deforming the material and eventually ends in fracture of the specimen. As is shown in Fig. 5 locking occurs at a ratio almost equal to 3, resulting to a value of N equal to 9. C_R is the rubbery or strain hardening modulus and can be calculated by differentiating

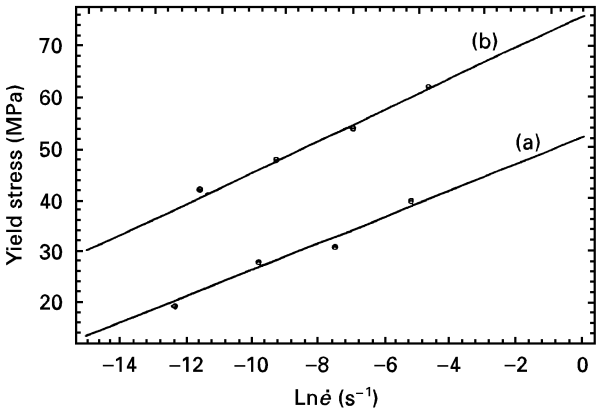

Figure 6 Yield stress versus logarithmic strain rate for (a) tensile and (b) compressive experiments.

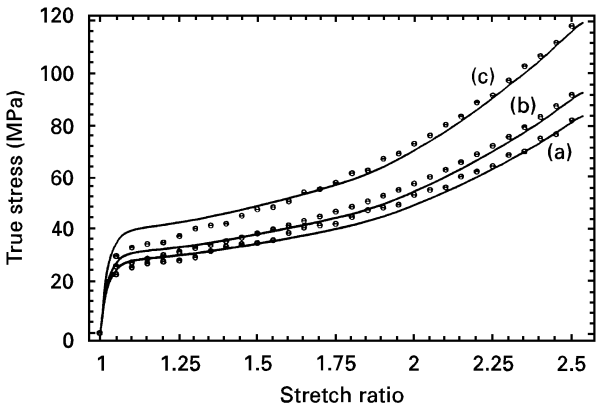

Figure 7 Tensile true stress–strain curves of polypropylene: theoretical results (points) versus experimental data (solid lines) at crosshead speeds of: (a) 0.1 mm min^{-1} (b) 1.0 mm min^{-1} and (c) 10 mm min^{-1}.

Equation 6 with respect to λ equal to 1.1 at the yield initiation. Therefore we have:

$$\frac{Y}{C_R} \geqslant 3.7 \tag{10}$$

Given that Y is equal to 26.5 MPa on average at the lower crosshead speeds, it can be shown that $C_R \leqslant 7.5$. The same procedure for the evaluation of C_R has also been followed by Haward [1].

Using the above mentioned parameter values, which have a specific molecular interpretation, it was possible to describe very accurately the whole true stress–strain curve for all crosshead speeds tested, as is shown in Fig. 7.

In an analogous manner, the engineering compressive stress–strain curves are presented in Fig. 8 for the three different crosshead speeds examined. These curves appear to have no strain softening, while yielding is exhibited by a different slope of the whole curve at a specific stretch ratio. The true stress–strain curves of Fig. 9 were constructed in a similar manner to the tensile ones, and with respect to the specific zone, that appears to have the maximum value of deformation. In the compression tests, the deformation distribution is almost the same along the three zones. Selecting the one with the slightly higher absolute values of deformation we obtain its time evolution in Fig. 10, for a crosshead speed of 0.1 mm min^{-1}. In this figure, a slight change in the slope is observed, when yielding occurs, which increases with time exhibiting a lower decreasing trend in respect to tensile test, at longer times. The corresponding curve of the true strain rate is shown in Fig. 11. It seems to be about one order of magnitude lower than the rate of the tensile experiment, exhibiting however, the same features, i.e., a peak value followed by a decreasing trend that is related to the hardening effect. In the case of compression there is no neck initiation, but rather the inverse effect of the broadening of the cross-sectional area.

The rate effect on the yield stress is again obvious, while the values of the compressive yield stresses are higher with respect to those of the tensile ones, for the same crosshead speeds. The corresponding straight line of yield stress versus logarithmic strain rate is

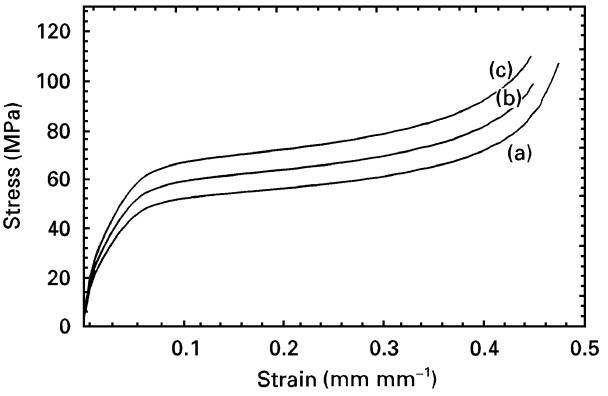

Figure 8 Engineering compressive stress–strain curves of polypropylene at crosshead speeds of: (a) 0.1 mm min^{-1}, (b) 1.0 mm min^{-1} and (c) 10 mm min^{-1}.

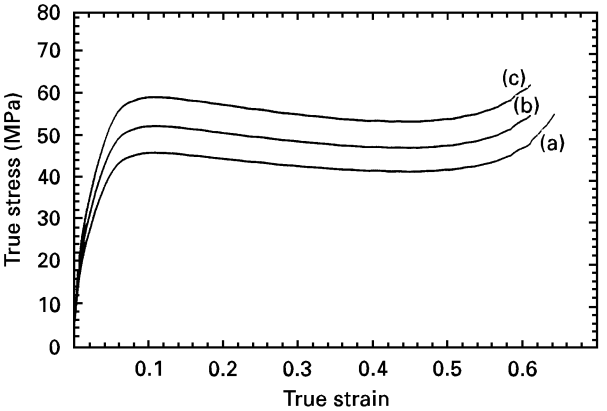

Figure 9 Compression true stress–strain curves of polypropylene at crosshead speeds of: (a) 0.1 mm min^{-1}, (b) 1.0 mm min^{-1} and (c) 10 mm min^{-1}.

shown in Fig. 6, defined with a different value for K_{kl} equal to 3.04 MPa for the case of compression test.

In all true stress–strain curves, a strain softening is observed, followed by a strain hardening at higher values of deformation. The amount of strain softening appears to be independent of the strain rate, as well as the strain hardening response at large strains, whilst locking (asymptotically increasing stress) occurs at a compressive strain approximately equal to −0.65.

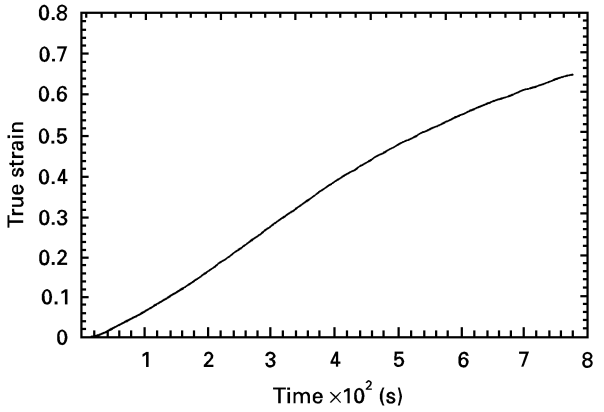

Figure 10 Strain variation versus time, for the zone with the maximum deformation, for a compression test at a crosshead speed of 0.1 mm min^{-1}.

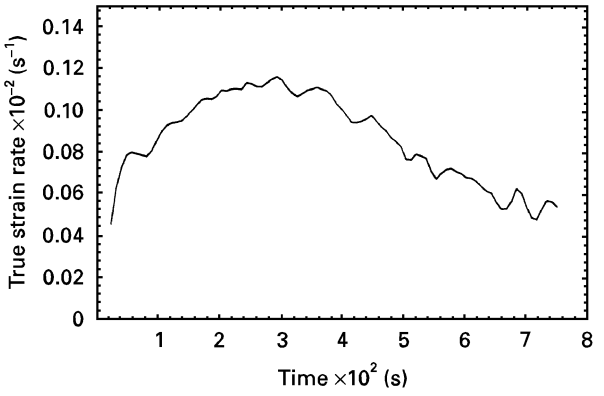

Figure 11 True strain rate versus time, obtained from the data of Fig. 10.

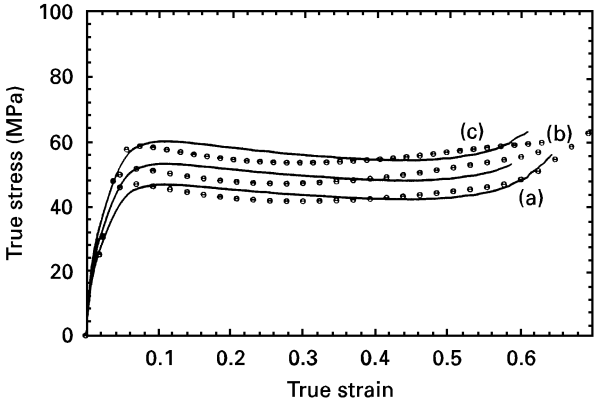

Figure 12 Compression true stress–strain curves of polypropylene: theoretical results (points) versus experimental data (solid lines) at crosshead speeds of: (a) 0.1 mm min^{-1}, (b) 1.0 mm min^{-1} and (c) 10 mm min^{-1}.

The rubber elastic stress can be modelled using the simpler Gaussian equation [22]. This suggestion seems to be reasonable for the case of moderate strains encountered during compression, where the Langevin relations may be reduced to the Gaussian form. The basic form of the Gaussian equation for moderate strains is:

$$\sigma_{ij} = Y + C_R\left(\lambda^2 - \frac{1}{\lambda}\right) \qquad (11)$$

where Y is the extrapolated yield stress, λ is the stretch ratio and C_R is the strain hardening modulus.

By differentiating Equation 11 with respect to λ equal to 0.95 (stretch ratio at which yielding occurs) we have:

$$\frac{Y}{C_R} = 2\lambda + \frac{1}{\lambda^2} \geqslant 3 \qquad (12)$$

Considering that the compressive yield stress is on average 50 MPa we obtain $C_R \leqslant 17$ MPa.

The numerical evaluation of Equation 5, for compression tests, has been made with a value of the pre-exponential factor of 7×10^{10} s as estimated from Fig. 6. The theoretical and experimental results are presented in Fig. 12, where a satisfactory agreement has been obtained.

4. Conclusions

A new experimental technique based on a non-contact method for longitudinal deformation measurement, has been used. A pattern code is applied onto the specimen along its gauge length, dividing it into zones. A laser beam scans the tape pattern code and its reflections are registered by a photocell. The reflections of the beam permit the strain and strain rate measurement at every zone, resulting in the deformation distribution along the gauge length.

Therefore, it was possible to detect the specific zone where neck initiation takes place, and to measure the inhomogeneous plastic deformation that is usually observed for semicrystalline polymers undergoing tensile testing.

In a similar way, the deformation distribution along the specimen gauge length in compression experiments was evaluated. In this case, a more uniform deformation distribution is observed. The exact measurement of strain provides the construction of the true stress–strain curves.

The theoretical description of the experimental results was made with the use of a non-linear viscoelastic model, and a good approximation has been obtained for both types of experiments at three different crosshead speeds. The parameter values used in our models have a specific molecular interpretation and are not simply curve fitting constants.

References

1. R. N. HAWARD, *J. Polym. Sci. B* **33** (1995) 1481.
2. A. SAWCZUK and G. BIANCHI, "Plasticity today" (Elsevier, London, 1985).
3. H. EYRING, *J. Chem. Phys.* **4** (1936) 283.
4. J. A. ROETLING, *Polymer* **6** (1965) 311.
5. *Idem, ibid* **7** (1966) 303.
6. T. REE and H. EYRING, *J. Appl. Polym. Sci.* **26** (1955) 793.
7. R. W. RENDELL, K. L. NGAI, G. R. FONG, A. F. YEE and R. J. BANKERT, *Polym. Engng Sci.* **27** (1987) 2.
8. R. M. SHAY JR. and J. M. CARUTHERS, *J. Rheol.* **30** (1986) 781.
9. J. M. LEFEBVRE and B. ESCAIG, *J. Mater. Sci.* **20** (1985) 438.
10. S. N. RUDNEV, D. B. SALAMATINA, V. V. VAENNIY and E. F. OLEINIK, *Colloid Polym. Sci.* **269** (1991) 460.

11. P. DUFFO, B. MONASSE, J. M. HAUDIN, C. G. SELL and A. DAHOUN, *J. Mater. Sci.* **30** (1995) 701.
12. E. KONTOU, *J. Appl. Polym. Sci.* **61** (1996) 2191.
13. T. S. CHOW, *J. Polym. Sci. B* **25** (1987) 137.
14. *Idem*, *Soc. Rheol.* **36**(8) (1992) 1707.
15. G. WILLIAMS and D. C. WATTS, *Trans. Faraday Soc.* **66** (1971) 80.
16. R. N. HAWARD and G. THACKRAY, *Proc. R. Soc. A* **302** (1968) 453.
17. D. M. PARKS, A. S. ARGON and B. BAGEPALLI, MIT Program in Polymer Science and Technology Report (1984).
18. M. C. BOYCE and E. M. ARRUDA, *Polym. Engng Sci.* **30**(20) (1990) 1288.
19. I. M. WARD, *ibid* **24** (1984) 724.
20. Y. Y. WANG and E. J. GUTH, *J. Chem. Phys.* **20** (1952) 1144.
21. M. C. BOYCE, D. M. PARKS and A. S. ARGON, *Mech. Mater.* **7** (1988) 15.
22. A. S. ARGON, *J. Macromol. Sci.* (*Phys.*) **B38** (1973) 573.

Received 23 July 1996
and accepted 18 July 1997